J Solid State Electrochem (2009) 13:1361–1366
DOI 10.1007/s10008-008-0696-y

ORIGINAL PAPER

Electrochemical properties of $LiFePO_4$/C synthesized using polypyrrole as carbon source

Sheng-Yao Chen · Bo Gao · Ling-Hao Su · Chang-Huan Mi · Xiao-Gang Zhang

Received: 7 July 2008 / Revised: 15 August 2008 / Accepted: 29 September 2008 / Published online: 17 October 2008

Abstract $LiFePO_4$/C composites were synthesized by pyrolysis of $LiFePO_4$/polypyrrole (PPy), which was obtained by an *in situ* chemical polymerization involving pyrrole monomer and hydrothermal synthesis $LiFePO_4$. All samples were characterized by X-ray diffraction, scanning electron microscopy, Fourier transform infrared spectroscopy, cyclic voltammetry, and galvanostatic charge–discharge techniques. The results showed the $LiFePO_4$/C sintered at 800 °C containing 2.8 wt.% carbon exhibited a higher discharge capacity of 49.6 $mAh{\cdot}g^{-1}$ at 0.1 C, and bare $LiFePO_4$ only delivered 11.6 $mAh{\cdot}g^{-1}$ in 2 M $LiNO_3$ aqueous electrolyte. The possible reason for the improvement of electrochemical performance was discussed and could be attributed to the formation of aromatic compounds during the carbonization of PPy.

Keywords $LiFePO_4$/C · Polypyrrole · Carbonization · Aqueous electrolyte

Introduction

Among the promising materials for positive electrodes of Li-ion rechargeable batteries, olivine $LiFePO_4$ has attracted huge interest since the pioneering work of Padhi et al. [1]. It has advantages of low toxicity, good thermal stability, and relatively high theoretical capacity as well as low cost. However, the poor inherent electronic conductivity and ion diffusivity become the obstacles for large-scale application in high power fields.

To overcome these drawbacks, several strategies have been reported to improve the rate capabilities of $LiFePO_4$ cathodes [2–5]. Among the methods for modifying $LiFePO_4$, carbon materials mixed or coated as the general approaches have been accepted [6, 7]. However, optimization of the cathode coating processes will be considered because new carbons have different physical characteristics. So far, the sources of carbon such as sucrose, glucose, carboxylic acid, and polypropylene have been regarded as effective exercise to control over the morphology, the size, the porous structure of carbon, and the formation of conductive phase for the conductivity improvement [8–11]. Ong et al. [12] have reported that the functionalized aromatic anhydrides or aromatic diketones as carbon sources improve the conductivity of $LiFePO_4$ cathodes. Additionally, Wang et al. [13] found polypyrrole–$LiFePO_4$ composite electrodes with an increased reversible capacity and better cyclability, compared to $LiFePO_4$ electrodes. Based on above thinking, we introduced the conducting polypyrrole as carbon source to obtain $LiFePO_4$/C composites by pyrolysis, during which the aromatic compounds were formed as a boost of conductivity. We investigated the improvement of electrochemical performance for the carbonized organic–inorganic composites at different temperatures, and obtained a remarkable augment of the specific capacity for $LiFePO_4$/C composites, compared to untreated $LiFePO_4$.

Yang and co-workers firstly found the hydrothermal synthesis of olivine iron phosphate [14, 15]. Herein, we synthesized olivine $LiFePO_4$ by the hydrothermal method and fabricated $LiFePO_4$/C composites by annealing $LiFePO_4$/PPy composites at various temperatures. To the best of our knowledge, there is no report on using conducting polypyrrole as carbon source to optimize carbon-mixed

S.-Y. Chen · B. Gao · L.-H. Su · C.-H. Mi · X.-G. Zhang (✉)
College of Material Science and Engineering,
Nanjing University of Aeronautics and Astronautics,
Nanjing, Jiangsu 210016, People's Republic of China
e-mail: azhangxg@163.com

$LiFePO_4$ composite so far. With this special carbon source, the carbon-mixed samples exhibited more excellent electrochemical properties than bare $LiFePO_4$ sample. The possible reasons for the enhanced electrochemical properties of $LiFePO_4$/C composite cathodes were discussed.

Experimental

The starting materials of this experiment were LiOH H_2O, $FeSO_4$ $7H_2O$, H_3PO_4, pyrrole (98%, Aldrich, distilled prior to usage), sodium *p*-toluenesulfonate, $FeCl_3$ $6H_2O$, and $LiNO_3$, etc. All of them were of A.R. grade and purchased from Shanghai Chemical Reagent Co. Ltd.

The lithium iron phosphate samples were prepared by a mild hydrothermal synthesis. $FeSO_4$ $7H_2O$ and H_3PO_4 were first dissolved into a purified water, and LiOH H_2O was added subsequently under vigor agitation. The molar ratio of Li:Fe:P was 2.5:1:1, and the concentration of $FeSO_4$ was controlled to be 0.1 M [16]. The resulting grayish green gel was transferred into a 120-ml capacity Teflon-lined stainless steel autoclave, sealed, and heated at 180 °C for 6 h. Precipitates were collected by suction filtration and dried at 110 °C for 2 h in a vacuum oven. The as-prepared powder showed light green.

The $LiFePO_4$/PPy composite was fabricated as follows: pyrrole (Py) monomer (0.1 ml), $LiFePO_4$ fine powder (500 mg), and a certain amount of sodium *p*-toluenesulfonate as doping agent and $FeCl_3$ $6H_2O$ as oxidant were dispersed in deionized water. The molar ratio of doping agent:Py:$FeCl_3$ was 1:3:9. The mixed solution was magnetically stirred at 5 °C for 24 h to complete the polymerization process. The final products were filtered, washed with deionized water, and dried at 110 °C in a vacuum oven for 2 h.

The $LiFePO_4$/C composites were fabricated by annealing the as-prepared $LiFePO_4$/PPy hybrid material at 600, 700, 800, 900, and 1,000 °C, abbreviating for $LiFePO_4$/C–X (X=600, 700, 800, 900, and 1,000) respectively. The $LiFePO_4$/PPy powder (1 g) was ball milled, and then was carbonized at above temperatures for 5 h in a tube furnace filled with argon (a heating rate of 5 $K \cdot min^{-1}$).

Phase purity of the synthesized materials was analyzed by X-ray diffraction (Bruker D8 advance, Germany) with Cu K_α radiation (λ=0.15418 nm) using a 2θ step of 0.02°. The particle morphology and structural properties of the samples were observed by a scanning electron microscopy (Quanta 200) operated at 20.0 kV. The carbon content of $LiFePO_4$/C-800 was evaluated by thermogravimetric analysis. Fourier transform infrared spectrometer was used to confirm the existence of aromatic rings in the pyrolysis product.

For electrochemical evaluation, galvanostatic charge–discharge test, cyclic voltammetry, and amplitude current (AC) impedance measurements were performed on CHI660B electrochemical workstation controlled by a personal computer. The electrode was prepared by pressing a powder mixture of the sample, acetylene black and poly (tetrafluoroethylene) (PTFE) (80:10:10, *w*/*w*/*w*). The active materials (10 mg) were pinched into Ni meshes as work electrodes, and then immersed into a three-electrode system of 2 M $LiNO_3$ solution. Saturated calomel electrode (SCE) and Pt electrode were used as reference and counter electrodes, respectively. The cells were galvanostatically charged and discharged between −0.4 and 0.6 V. All the electrochemical measurements were performed at ambient temperature (25±1 °C).

Results and discussion

XRD analysis of $LiFePO_4$, $LiFePO_4$/PPy, and $LiFePO_4$/C

The X-ray diffraction patterns of as-synthesized $LiFePO_4$ powders, $LiFePO_4$/PPy composite, and $LiFePO_4$/C obtained by heat treating at 600–1,000 °C are shown in Fig. 1. Olivine $LiFePO_4$ was synthesized by hydrothermal reaction without using any reductant. The molar ratio of Li:Fe:P=2.5:1:1 in the starting solution was employed to obtain single phase of $LiFePO_4$ [16]. All patterns except for the $LiFePO_4$/PPy agree well with that of phospho-olivine $LiFePO_4$, and the unidentified phase is labeled by a dot. Main peaks for $LiFePO_4$ are labeled with *h k l* indexes. The diffraction profile is identified to be the ordered olivine structure and indexed by the space group of orthorhombic Pnma, in which the Li ions occupy the octahedral sites (4a); Fe atoms occupy the octahedral sites (4c); and P atoms occupy tetrahedral sites (4c) [17]. The lattice parameters of $LiFePO_4$, calculated by XRD data (Fig. 1), are a= 10.332 Å, b=6.010 Å, and c=4.692 Å, respectively; these

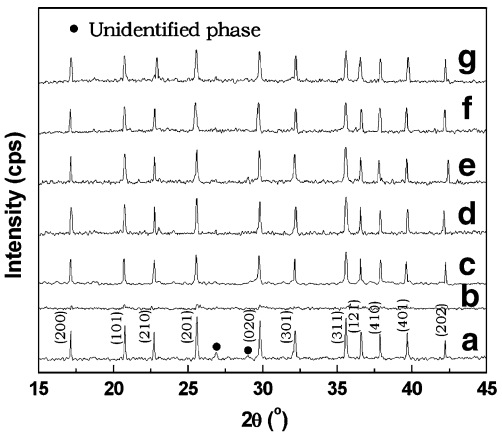

Fig. 1 XRD patterns of hydrothermally synthesized $LiFePO_4$ (**a**), $LiFePO_4$/PPy (**b**), and carbonized samples (**c**)–(**g**) heated at 600, 700, 800, 900, and 1,000 °C, respectively

values are very close to the standard data (a=10.33 Å, b=6.010 Å, and c=4.693 Å) given by JCPDS, card 83-2092. With very sharp peaks, it suggested a high crystallization, even though the product was prepared at a relatively low temperature of 180 °C. The peak intensities of $LiFePO_4$/PPy composite presented in Fig. 1b are obviously weaker than any other one, indicating the formation of an amorphous phase encompassing $LiFePO_4$ particles during *in situ* polymerization. XRD patterns of $LiFePO_4$/C, which was obtained by annealing $LiFePO_4$/PPy under argon atmosphere from 600 to 1,000 °C, are shown in Fig. 1c–g. The heat-treated process makes the amorphous phase coating decomposition or transformation. Though the annealed samples still maintain the standard pattern of olivine $LiFePO_4$, their peak intensities of XRD data are smaller than the $LiFePO_4$. These results indicate the formation of new carbonaceous material after annealing.

SEM analysis of $LiFePO_4$, $LiFePO_4$/PPy, and $LiFePO_4$/C-800

The SEM images of $LiFePO_4$, $LiFePO_4$/PPy, and $LiFePO_4$/C-800 could be seen from Fig. 2a,b,c, and d, respectively. The as-synthesized $LiFePO_4$ particles typically showed rhombus shape, and aggregated like a coarse ball (see Fig. 2c), which consisted well with that reported by Yang et al. [14]. The particle size of bare $LiFePO_4$ was ca. 10 μm (see Fig. 2a). PPy was introduced into $LiFePO_4$ by chemical oxidation polymerization, during which the positive charges of polarons or bipolarons appeared. The morphology of $LiFePO_4$/PPy composite was shown in Fig. 2b, from which it could be seen PPy coated the $LiFePO_4$ particles uniformly. The electro-neutrality of PPy was maintained by incorporating with doping anions. The polymerization reaction could be expressed in Eq. (1).

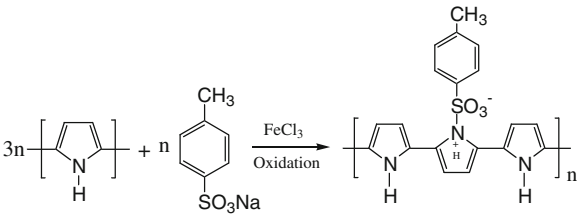

(1)

where (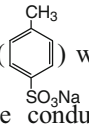) was the counter-ion, which was incorporated into the conducting polymer chains during reactions; n delegated the molecular weight [13]. The electrical conductivity of the PPy was improved by the intrachain transport of the polarons or bipolarons. Polymer chains also could be

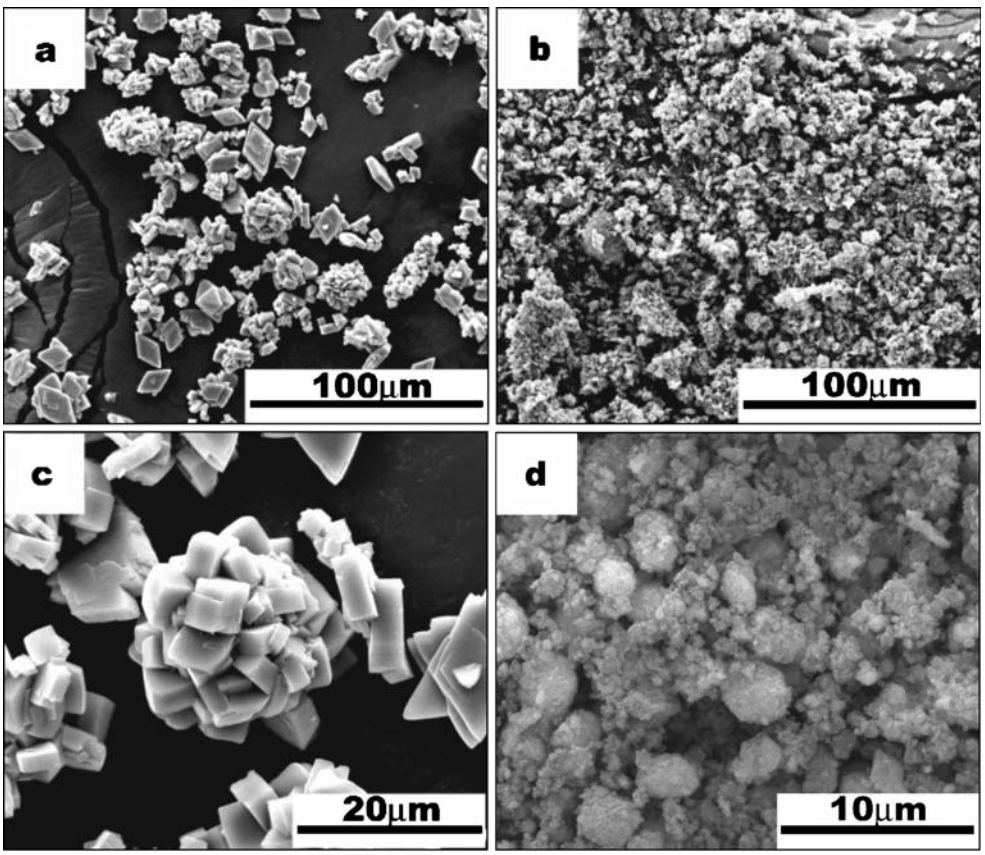

Fig. 2 SEM images of $LiFePO_4$ (**a**, **c**), $LiFePO_4$/PPy (**b**), and $LiFePO_4$/C-800 (**d**)

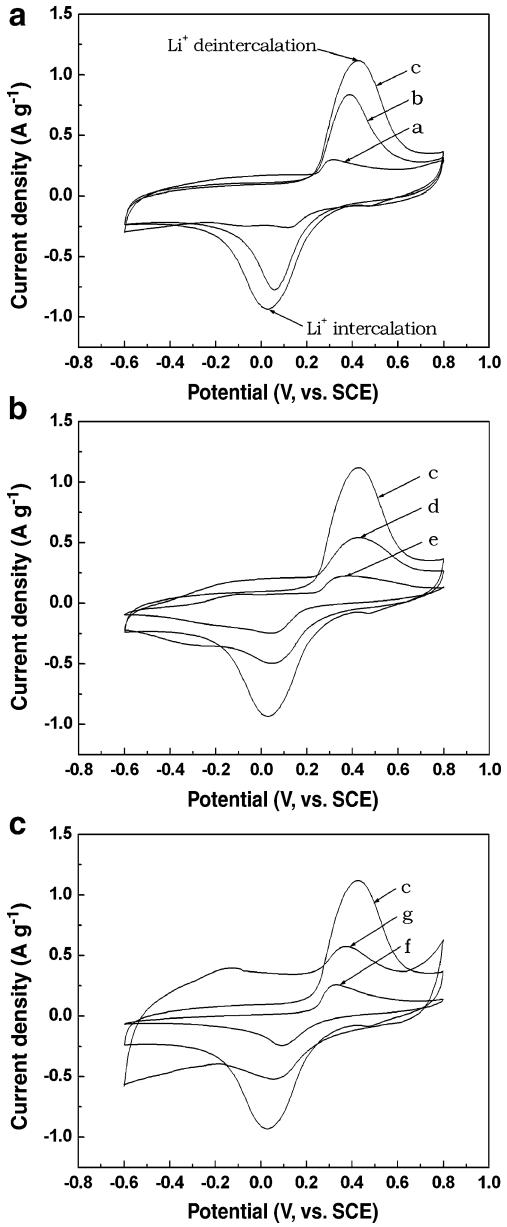

Fig. 3 Cyclic voltammograms of $LiFePO_4$/C-600 (**a**), $LiFePO_4$/C-700 (**b**), $LiFePO_4$/C-800 (**c**), $LiFePO_4$/C-900 (**d**), $LiFePO_4$/C-1000 (**e**), $LiFePO_4$ (**f**), and $LiFePO_4$/PPy (**g**) at a scan rate of 1 mV s^{-1}. All load mass are 5 mg

further doped with counter-ions originating from either oxidant (e.g., $FeCl_3$) or dopant [18]. For $LiFePO_4$/C composites, they were obtained by carbonizing $LiFePO_4$/PPy composite at 600–1,000 °C. The image of $LiFePO_4$/C sintered at 800 °C was shown in Fig. 2d. It was clear to see that mass amount of carbonaceous material was formed on $LiFePO_4$ particles due to the decomposition of PPy during pyrolysis. This carbonaceous coating on $LiFePO_4$ could be speculated to improve the electrical conductivity of $LiFePO_4$.

Electrochemical behavior of $LiFePO_4$, $LiFePO_4$/PPy, and $LiFePO_4$/C

The cyclic voltammograms of $LiFePO_4$, $LiFePO_4$/PPy, and all $LiFePO_4$/C composites in 2 M $LiNO_3$ aqueous solution are given in Fig. 3a,b, and c. It can be seen that a pair of Li-ion intercalation and deintercalation peaks can be observed under a safe potential window between −0.6 V and 0.8 V. The increasing peak current can be observed from 600 °C to 800 °C (see Fig. 3a), whereas a descend is exhibited from 800 to 1,000 °C (see Fig. 3b) under a fixed redox peak potential. The redox peak current of $LiFePO_4$/C-800 is highest among all $LiFePO_4$/C composites, shown in Fig. 3a and b, suggesting that $LiFePO_4$/C-800 has the best electrochemical activity. Fig. 3c presents a comparison of the CV curves among the bare $LiFePO_4$, $LiFePO_4$/PPy, and $LiFePO_4$/C-800 electrodes. From the redox peak current value, the $LiFePO_4$/PPy electrode showed an improvement of the electrochemical activation, compared to bare $LiFePO_4$ electrode. However, the peak current density of $LiFePO_4$/C-800 (1.12 $A{\cdot}g^{-1}$, oxidation potential vs. SCE) greatly exceeds that of $LiFePO_4$/PPy (0.57 $A{\cdot}g^{-1}$, oxidation

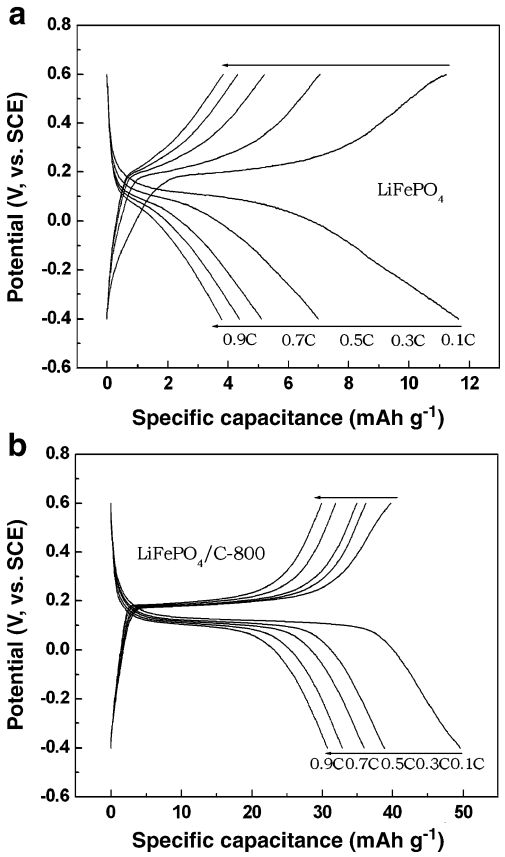

Fig. 4 Charge–discharge test of $LiFePO_4$ and $LiFePO_4$/C-800 between −0.4 V and 0.6 V at 0.1 C, 0.3 C, 0.5 C, 0.7 C, and 0.9 C, respectively

potential vs. SCE) and $LiFePO_4$ (0.25 $A \cdot g^{-1}$, oxidation potential vs. SCE). These results show that the optimal heat-treated temperature is 800 °C. It is noticeable that the cyclic profile of $LiFePO_4$/PPy is appreciably in disaccord with the profile of $LiFePO_4$, which may be attributed to the Li^+ insertion/extraction reaction of PPy.

Figure 4a and b shows the charge–discharge curves of bare $LiFePO_4$ and $LiFePO_4$/C-800 electrode. The $LiFePO_4$/C-800 with remarkable charge–discharge plateaus presents better than bare $LiFePO_4$ electrode in capacitance and rate capability. The specific capacity of $LiFePO_4$/C-800 for the first cycle can be reached 49.6 $mAh \cdot g^{-1}$ at 0.1 C, which is much larger than that of bare $LiFePO_4$ electrode (only 11.6 $mAh \cdot g^{-1}$). Even at 0.9 C, $LiFePO_4$/C-800 delivers 30.8 $mAh \cdot g^{-1}$, which is also larger than the specific capacitance of bare $LiFePO_4$ electrode (3.8 $mAh \cdot g^{-1}$). The calculation of specific capacity can be based on the following equation:

$$C = I\,\Delta t/(3600 \cdot m) \tag{2}$$

where C is the capacity ($mAh \cdot g^{-1}$), I is the current density of charge–discharge (mA), Δt is the time interval of each discharge (s), and m is the mass of active material (g). Compared to the results in the aqueous electrolyte reported by He et al. [19], the results obtained by us are slightly undesirable, but the great improvement of capacity after pyrolysis is unexpected and recommendable, indicating a feasible method to carbon-mixed $LiFePO_4$ by annealing the precursor with conducting polymer. Furthermore, the size of $LiFePO_4$ particles may mostly be responsible for the depressing results.

AC impedance measurement was applied to test the electric conductivity of the untreated $LiFePO_4$ and $LiFePO_4$/C-800 composite electrodes. Before test, both electrodes were cycled galvanostatically for ten cycles to ensure the stable formation of SEI films on the surface of the electroactive particles. Figure 5 gives typical Nyquist plots of the bare $LiFePO_4$ and $LiFePO_4$/C-800 composite electrodes. The spectra show an intercept at high frequency, a depressed semicircle in the high-middle frequency region, and a straight line in the low frequency region. The intercept impedance on the Z' axis represents the ohmic resistance, which contains the resistance of the aqueous electrolyte and active electrode. The high frequency region of the semicircle represents the migration of the Li^+ ions at the electrode/electrolyte interface through the SEI films, whereas the middle frequency range of the semicircle corresponds to the charge-transfer process. The low frequency region of the straight line is attributed to the diffusion of the lithium ions into the bulk of the electrode material or so-called Warburg diffusion. According to the comparison of high-middle frequency region of both electrodes, the semicircle radius of $LiFePO_4$/C-800 is smaller than

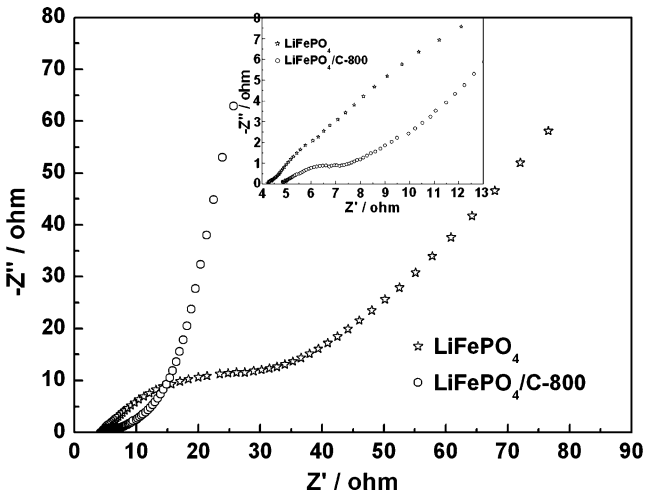

Fig. 5 AC impedance spectra of bare $LiFePO_4$ electrode (*pentacle*) and $LiFePO_4$/C-800 electrode (*circle*). *Inset* shows the amplificatory shape of low frequency region

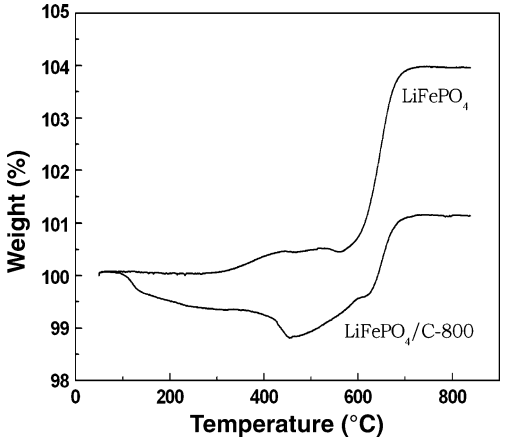

Fig. 6 Thermogravimetric curves for the $LiFePO_4$/C-800 composite and $LiFePO_4$. Heating rate was 5 K min^{-1}

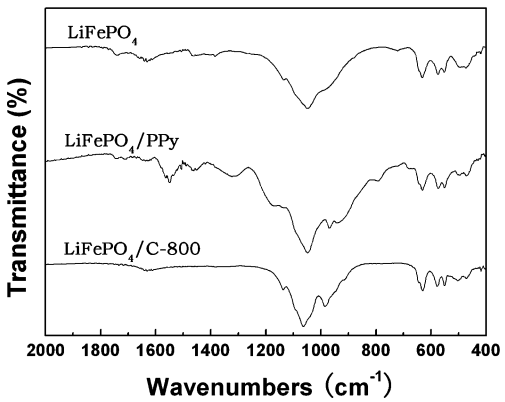

Fig. 7 Fourier transform infrared (FT-IR) spectra for $LiFePO_4$, $LiFePO_4$/PPy, and $LiFePO_4$/C-800

that of bare $LiFePO_4$, indicating that the electric conductivity of the former is better.

Analysis of possible reasons

The weight ratio of carbon was determined by heating the untreated $LiFePO_4$ and $LiFePO_4$/C-800 in oxygen gas (see Fig. 6). The difference of weight change in the $LiFePO_4$/C-800 composites and $LiFePO_4$ denoted the mass of carbon content in the composites because the carbon in the composites was burned off by heating in oxygen gas till 850 °C [14]. Figure 6 shows that bare $LiFePO_4$ gains 3.96% in weight, compared to the theoretical value of 5.1% for complete oxidation of Fe(II) to Fe(III). The mass of $LiFePO_4$/C-800 composite gains only 1.14%, giving a carbonization level of 2.82 wt.%.

For $LiFePO_4$/C-800 fired at 800 °C under Ar gas, the loss of N atoms occurs mainly between 400 and 600 °C [20]. With the loss of N atoms, polycondensed aromatic hydrocarbons formed, and the increase in the radical species formed in carbonization reactions provides a high electric conductivity. Meanwhile, amorphous carbon may be responsible for the high electric conductivity [20].

The FT-IR spectra of untreated $LiFePO_4$, $LiFePO_4$/PPy, and $LiFePO_4$/C-800 are shown in Fig. 7. The intramolecular vibrations of the connected PO_4 tetrahedra appear in the wavenumber range of 372–1,139 cm^{-1} [21]. Both symmetric and antisymmetric O–P–O bending modes exist in the range of 372–647 cm^{-1}. Symmetric and antisymmetric P–O stretching modes exist in the range of 945–1,139 cm^{-1} [21]. These bending and stretching modes in all samples were observed (see Fig. 7). The main differences between $LiFePO_4$ and $LiFePO_4$/PPy are the appearance of the band (1,474 and 1,189 cm^{-1}) assigned to the C–N stretching vibration, the band (1,554 cm^{-1}) attributed to the C=C stretching vibration, and the weak band around 1,705 cm^{-1} corresponded to the C=O stretching, which suggests that the pyrrole rings were slightly overoxidized. The bands at 1,297 and 926 cm^{-1} may be assigned to the doped bands [22]. This also demonstrates the successful incorporation between $LiFePO_4$ and PPy. For the IR spectroscopy of $LiFePO_4$/C-800, the characteristic bands of aromatic compounds appear around 1,600 cm^{-1}, which contribute to increase electrical conductivity [20].

Conclusions

The polypyrrole as a carbon source was successfully composed with olivine $LiFePO_4$ to obtain $LiFePO_4$/C material by a pyrolysis process. Electrochemical test showed that $LiFePO_4$/C obtained at 800 °C delivered a specific capacity of 49.6 $mAh \cdot g^{-1}$, which is much higher than that of untreated $LiFePO_4$ (11.6 $mAh \cdot g^{-1}$). The improvement of electrochemical performance was mainly contributed to the formation of the aromatic groups in $LiFePO_4$/C. This is a promising strategy using conducting polymers as carbon sources to fabricate carbon mixed or coated cathode materials with the electrochemical improvement.

Acknowledgments This work was supported by National Basic Research Program of China (973 Program) (No. 2007CB209700), National Natural Science Foundation of China (No.20633040), and Natural Science Foundation of Jiangsu Province (BK2006196).

References

1. Padhi K, Nanjundaswamy KS, Goodenough JB (1997) J Electrochem Soc 144:1188. doi:10.1149/1.1837571
2. Huang YH, Park KS, Goodenough JB (2006) J Electrochem Soc 153:A2282. doi:10.1149/1.2360769
3. Park KS, Schougaard SB, Goodenough JB (2007) Adv Mater 19:848. doi:10.1002/adma.200600369
4. Mi CH, Zhang XG, Li HL (2007) J Electroanal Chem 602:245. doi:10.1016/j.jelechem.2007.01.007
5. Hu YS, Guo YG, Dominko R, Gaberscek M, Jamnik J, Maier J (2007) Adv Mater 19:1963. doi:10.1002/adma.200700697
6. Salah AA, Mauger A, Zaghib K, Goodenough JB, Ravet N, Gauthier M (2006) J Electrochem Soc 153:A1692. doi:10.1149/1.2213527
7. Chiu KF (2007) J Electrochem Soc 154:A129. doi:10.1149/1.2404898
8. Liao XZ, Ma ZF, He YS, Zhang XM, Wang L, Jiang Y (2005) J Electrochem Soc 152:A1969. doi:10.1149/1.2008988
9. Gao F, Tang ZY, Xue JJ (2007) Electrochim Acta 53:1939. doi:10.1016/j.electacta.2007.08.048
10. Fey GTK, Lu TL (2008) J Power Sources 178:807. doi:10.1016/j.jpowsour.2007.09.039
11. Mi CH, Zhang XG, Zhao XB, Li HL (2006) J Alloy Comp 424:327. doi:10.1016/j.jallcom.2005.12.062
12. Ong CW, Lin YK, Chen JS (2007) J Electrochem Soc 154:A527. doi:10.1149/1.2720714
13. Wang GX, Yang L, Chen Y, Wang JZ, Bewlay S, Liu HK (2005) Electrochim Acta 50:4649. doi:10.1016/j.electacta.2005.02.026
14. Yang SF, Zavalij PY, Whittingham MS (2001) Electrochem Commun 3:505. doi:10.1016/S1388-2481(01)00200-4
15. Yang SF, Song YN, Zavalij PY, Whittingham MS (2002) Electrochem Commun 4:239
16. Shiraishi K, Dokko K, Kanamura K (2005) J Power Sources 146:555. doi:10.1016/j.jpowsour.2005.03.060
17. Andersson AS, Kalska B, Haggstrom L, Thomas JO (2000) Solid State Ion 130:41. doi:10.1016/S0167-2738(00)00311-8
18. Kuhn HH, Child AD, Kimbrell WC (1995) Synth Met 71:2139. doi:10.1016/0379-6779(94)03198-F
19. He P, Zhang X, Wang YG, Cheng L, Xia YY (2008) J Electrochem Soc 155:A144. doi:10.1149/1.2815609
20. Ando E, Onodera S, Iino M, Ito O (2001) Carbon 39:101. doi:10.1016/S0008-6223(00)00098-1
21. Burba CM, Frech R (2004) J Electrochem Soc 151:A1032. doi:10.1149/1.1756885
22. Geng WC, Li N, Li XT, Wang R, Tu JC, Zhang T (2007) Sensors Actuators B 125:114. doi:10.1016/j.snb.2007.01.041